Polymer 51 (2010) 4419–4423

Contents lists available at ScienceDirect

Polymer

journal homepage: www.elsevier.com/locate/polymer

Nanostructured silica-type hybrids from poly(styrene-*b*-ethylene oxide-*b*-caprolactone) copolymers

Jie Song [a], Jin-Woo Choi [a], Eunji Lee [b], Jeong-Kyu Lee [c], Wang-Cheol Zin [c], Byoung-Ki Cho [a,*]

[a] Department of Chemistry and Institute of Nanosensor and Biotechnology, Dankook University, Gyeonggi-Do, 448-701, Republic of Korea
[b] Department of Chemistry, Yonsei University, Seoul, 120-749, Republic of Korea
[c] Department of Materials Science and Engineering, Pohang University of Science and Technology, Pohang, 790-784, Republic of Korea

ARTICLE INFO

Article history:
Received 5 April 2010
Received in revised form
13 July 2010
Accepted 14 July 2010
Available online 21 July 2010

Keywords:
Block copolymers
Morphology
Nanocomposites

ABSTRACT

By employing a triblock copolymer, poly(styrene-*b*-ethylene oxide-*b*-caprolactone) copolymer, as a structure-directing agent, a series of silica-type hybrid materials were prepared via a sol-gel method of (3-glycidyloxypropyl) trimethoxy silane and aluminum *sec*-butoxide. Small angle X-ray scattering and transmission electron microscopy analyses demonstrated that ordered nanostructures, from lamellar to 2-dimensional hexagonal columnar with a disordered intermediate morphology, were exhibited as a function of the amount of loaded silica nanoparticles. Among the observed morphologies, the silica particles in the lamellar sample were localized at the PS/PEO interface, which could be elucidated by the dominant translational entropy of small silica particles.

1. Introduction

Block copolymer/nanoparticle hybrids, so-called nanocomposites, have received a great deal of attention because of their diverse applications, such as catalysts, fuel cells, photonic band gap materials and porous membranes [1,2]. The locations of nanoparticles are dictated by the self-assembly of the block copolymer, by which the material natures of nanocomposites such as optical and conducting properties can be tuned [3,4]. For the past decade, the parameters influencing the particle ordering in composites have been investigated. For example, in the easiest approach, the surface tailoring of nanoparticles has been attempted to increase the compatibility with one polymer block [5–8]. Recently, the size of the nanoparticle was revealed to be very crucial to designating the particle location. According to a theoretical work by the Balazs group [9,10], the particle size-dependent co-assembling behavior was determined by competing two entropic factors, one translational and one conformational. Regarding this research topic, several experimental efforts have been made, and they mostly adopted the simplest diblock copolymer system [11–14]. On the other hand, more recently, the Wiesner group reported the nanocomposites using triblock copolymers [15,16]. As a result, they proved that unconventional morphologies such as "pillared-lamellae" and "woodpile" structures could be made using the triblock copolymers. Nevertheless, more experimental evidence should be gained to generalize the nanocomposite system from triblock copolymer assemblies.

Polystyrene-*b*-poly(ethylene oxide)-*b*-poly(ε-caprolactone)(PS-*b*-PEO-*b*-PCL) copolymers contain two crystalline blocks, by which their nano-segregated morphologies are particularly interesting in the crystalline states. Regarding these triblock copolymers, several groups have studied on the crystallization and morphological behaviors. Floudas et al. investigated the phase behavior of star-like PS-*b*-PEO-*b*-PCL copolymers [17]. They reported that the microphase separation occurred mainly due to the crystallization of one or both crystallizable blocks from the homogeneous disordered phase, and the coil length ratio of PEO and PCL was described as the dominant parameter for the determination of the block crystallization. Recently, Arnal et al. reported on the detailed thermal properties (i.e., crystallization and melting) of linear PS-*b*-PEO-*b*-PCL copolymers using a self-nucleation technique [18,19]. They demonstrated that the confinement of the crystallizable blocks by the vitreous PS block governed the self-nucleation behavior of the triblock copolymers. As a result, they concluded that during the crystallization process, degree of the supercooling was greater in a cylindrical morphology with a PS matrix than a layered structure.

Here, we reported a morphological transition of silica-type hybrid materials from lamellar to hexagonal columnar structures

* Corresponding author. Tel.: +82 31 8005 3153; fax: +82 31 8005 3148.
E-mail address: chobk@dankook.ac.kr (B.-K. Cho).

0032-3861/$ – see front matter © 2010 Elsevier Ltd. All rights reserved.
doi:10.1016/j.polymer.2010.07.020

with a disordered intermediate one. In this study, we synthesized a PS-*b*-PEO-*b*-PCL copolymer by using sequential anionic and ring-opening polymerizations (Scheme 1), and for the first time utilized this as a structure-directing agent for the preparation of hybrid materials. In this work, we examined the hybrid system at both high and low particle concentration regimes, by which we wanted to see the influence of the crystallizable blocks on the hybrid formation. Regarding this, we described in this paper the structural variations of the hybrid materials, such as morphological and dimensional changes.

2. Experimental section

2.1. Materials

n-Butyllithium (2.5 M solution in hexanes), *sec*-butyllithium (1.4 M solution in cyclohexane), ethylene oxide, 1,1-diphenylethylene, methanolic HCl (1.25 M in methanol) and triethyl aluminum (1.9 M solution in toluene) were purchased from Sigma–Aldrich Chemical Co. ε-Caprolactone (Aldrich) and pyridine were dried over CaH_2 for 48 h and freshly distilled under reduced pressure just before use. Styrene (Aldrich) and dichloromethane were dried individually in the presence of CaH_2 for 48 h, and transferred to a flame-dried graduated ampoule under vacuum. Tetrahydrofuran (THF) and cyclohexane were dried with deep red 1,1-diphenyl ethylene/*n*-butyllithium adduct, and degassed several times before distillation into a flame-dried schlenk flask under vacuum. In addition, ethylene oxide was stirred over n-butyllithium at 0 °C, distilled into a graduated ampoule and stored at −20 °C. In the calculation of the cross-sectional area of a single PS coil in the layer structure, the densities were used to be 1.04 g/cm^3, 1.05 g/cm^3, 1.14 g/cm^3, and 2.2 g/cm^3 for PS, PEO, PCL, and silica, respectively.

2.2. Methods

^{1}H NMR spectra were recorded on Varian 500 instrument, using chloroform-*d* ($CDCl_3$) as the solvent, and tetramethylsilane (TMS) as the internal reference for chemical shifts. Gel permeation chromatography (GPC) determinations were performed on a waters system equipped with a Waters 510 HPLC pump, a Waters M486 tunable absorbance detector, a Waters M410 differential refractive index detector and three waters styragel HR columns with a continuous porosity of 10^2–10^4 Å. Monodisperse linear polystyrene standards were used for the preparation of the calibration curve. THF (with 2% v/v *N*,*N*-dimethylacetamide) was used as the eluent at a rate of 1.0 mL/min at 35 °C. The purity of the products was checked using thin-layer chromatography (TLC; Merck, silica gel 60). A Perkin Elmer Pyris6 differential scanning calorimetry (DSC) was used to determine thermal transitions, which were reported as the maxima of their endothermic peaks. In all cases, heating scans were measured at a rate of 5 °C/min. X-ray scattering measurements were performed in transmission mode with synchrotron radiation at the 10C1 X-ray beam line of the Pohang Accelerator Laboratory, Korea. The sample was held in an aluminum sample holder with films on both sides. For transmission electron microscopy (TEM) analysis, the electron transparent films of the hybrid materials with a thickness of 70–120 nm were microtomed using a RMC PowerTome-XL with a glass knife, and were then transferred to carbon-coated Cu-grid substrates. The TEM measurements were performed at 120 kV using JEM-2010.

2.3. Synthesis

An intermediate poly(styrene-*b*-ethylene oxide) (**PS-*b*-PEO**) copolymer was synthesized using an anionic polymerization described in a previous publication [20].

2.3.1. Hydroxy-terminated polystyrene

^{1}H NMR (500 MHz, $CDCl_3$, ppm): δ = 1.30–0.53 (−CH(phenyl) $CH_2CH(CH_2CH_3)CH_3$), 1.90–1.31 (CH_2 of the PS backbone), 2.61–1.90 (*CH* of the PS backbone), 3.30 ($HOCH_2CH_2$−), 7.38–6.36 (aromatic). TLC (eluent; hexane/CH_2Cl_2 = 2:3): R_f = 0.46. M_n (from NMR) = 20 800 g/mol. M_w/M_n (from GPC) = 1.02.

2.3.2. Poly(styrene-b-ethylene oxide) copolymer (PS-b-PEO)

^{1}H NMR (500 MHz, $CDCl_3$, ppm): δ = 1.30–0.53 (−CH(phenyl) $CH_2CH(CH_2CH_3)CH_3$), 1.90–1.31 (CH_2 of the PS backbone), 2.61–1.90 (*CH* of the PS backbone), 3.82–3.45 ($-CH_2CH_2O-$), 7.38–6.36 (aromatic). TLC (eluent; CH_2Cl_2/methanol = 8:1): R_f = 0.49. M_n (from NMR) = 25 800 g/mol, M_w/M_n (from GPC) = 1.05.

2.3.3. Synthesis of poly(styrene-b-ethylene oxide-b-caprolactone) copolymer (PS-b-PEO-b-PCL)

To a solution of **PS-*b*-PEO** (3.0 g, 0.13 mmol) in 60 mL of dichloromethane under nitrogen, $AlEt_3$ (1.9 M solution, 74.2 μL, 0.14 mmol) and pyridine (11.4 μL, 0.14 mmol) were added. The reaction mixture was stirred vigorously at room temperature for 3 h. Next, caprolactone (1.6 g, 14.1 mmol) was inserted into the reaction mixture, and the solution was then stirred vigorously at room temperature for 42 h. The polymerization was quenched by adding 2 equiv. HCl (1.25 M solution, 0.23 mL) and the solution was poured in excess of methanol. Finally, by carrying out the precipitation three times using methanol, the triblock copolymer (3.4 g) was isolated as a white solid. ^{1}H NMR (500 MHz, $CDCl_3$, ppm): δ = 1.30–0.53 (−CH(phenyl)$CH_2CH(CH_2CH_3)CH_3$), 1.43–1.28 (−OOC−CHCH*CH*CHCHO−), 1.65–1.50 (−OOC−CH(CH_3)−), 1.71–1.51 (−OOC−CH*CH*CH*CH*CH−), 1.90–1.31 (CH_2 of the PS backbone), 2.40–2.24 (−OOC−*CH*CHCHCHCH−), 2.61–1.90 (*CH* of the PS backbone), 3.82–3.45 ($-CH_2CH_2O-$), 4.15–3.98 (−OOC−CHCHCHCH*H*−), 7.38–6.36 (aromatic). TLC (eluent; CH_2Cl_2/methanol = 8:1): R_f = 0.49. M_n (from NMR) = 33 800 g/mol, M_w/M_n (from GPC) = 1.09.

3. Results and discussion

3.1. Preparation and characterization of poly(styrene-b-ethylene oxide-b-caprolactone) copolymer (PS-b-PEO-b-PCL)

As a structure-directing agent, a triblock copolymer, **PS-*b*-PEO-*b*-PCL**, was prepared through sequential anionic and ring-opining polymerizations. The synthesis of poly(styrene-*b*-ethylene oxide) (**PS-b-PEO**) was accomplished via a two-step anionic polymerization of styrene and ethylene oxide monomers. The synthetic details were described previously [20]. The third block, polycaprolactone, could be introduced by a ring-opening polymerization (Scheme 1).

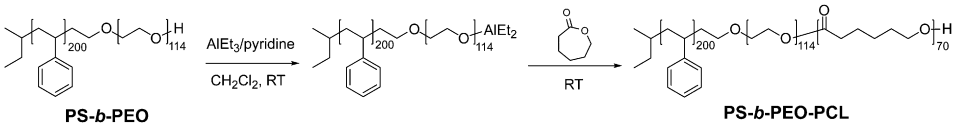

Scheme 1. Ring-opening polymerization of caprolactone for the preparation of **PS-*b*-PEO-*b*-PCL**.

In this step, the PS-*b*-PEO-O-$AlEt_2$ macroinitiator was prepared from an $AlEt_3$/pyridine system in dichloromethane, and the polymerization of caprolactone was performed at room temperature. Pyridine was used to inhibit the chelation of oxygen atoms in PEO to aluminum; otherwise, caprolactone monomers hardly approached aluminum center [21]. The resulting block copolymer showed a narrow molecular weight distribution of 1.09, as measured by gel permeation chromatography (GPC). From the ^{1}H NMR analysis, the molecular weights (M_n) for the PS, PEO and PCL blocks were determined to be approximately 20 800 g/mol, 5000 g/mol and 8000 g/mol, respectively. The differential scanning calorimetry (DSC) data revealed two melting transitions at 31.8 °C and 52.7 °C for the PEO and PCL blocks, and the PS glass transition at 88.2 °C (Fig. 1(a)). The nanostructure of the block copolymer was investigated by small and wide angle X-ray scattering (SAXS and WAXS) methods. The SAXS data at 25 °C exhibited an intense peak and weak shoulder-like reflections (Fig. 1(b)). Although the morphological interpretation in this case was not so clear due to the broad reflections, this SAXS data could be assigned as a hexagonal columnar structure with its inter-columnar distance of 33.0 nm. Indeed, a linear PS-*b*-PEO-*b*-PCL copolymer with the comparable weight fraction of each block (63%, 16% and 21% for PS, PEO and PCL, respectively) reported by the Müller group, also exhibited a hexagonal columnar morphology in the crystalline state, which may confirm our morphology assignment [19]. In contrast to the ordered columnar structure, the SAXS reflections disappeared above the PS glass transition temperature (T_g), which indicates no ordered phase in the melt (Fig. 1(b)). Therefore, we assumed that the morphology in the crystalline state was attributed to the crystallization of the PCL block. Actually, the freshly air-cooled sample from the melt did not display any assignable peak in the SAXS data. However, after a long-time annealing at room temperature (RT) for more than 48 h, the ordered SAXS pattern was revived, together with the typical WAXS reflections of the crystalline PCL block at $2\theta = 21.4^\circ$ and 23.7° (Fig. 1(c)) [22]. This means that a large supercooling occurred in the crystallization process. This supercooling behavior was corroborated by a polarized optical microscopy (POM) analysis. On the first heating, the strong birefringence at RT disappeared at the PCL melting temperature of 53 °C, and the optically isotropic brittle sample became a viscous liquid at near T_g of the PS. Upon the subsequent cooling, the optical behavior did not change over the entire temperature range from the liquid state to RT. However, a long-time annealing at RT yielded a considerable birefringence coming from the PCL crystallization. The occurrence of the supercooling could be attributed to the hard confinement of the crystallizable blocks within the vitreous PS matrix, by which it might be difficult to nucleate every isolated microdomain [19].

3.2. Silica-type hybrids by the co-assembly of silica nanoparticles and triblock copolymers

By loading different amounts of prehydrolyzed sol nanoparticles of (3-glycidyloxypropyl) trimethoxy silane and aluminum *sec*-butoxide to **PS-*b*-PEO-*b*-PCL**, we prepared three hybrid materials, **1**–**3**, as bulk films [23]. The weight fractions (f_w) of the loaded inorganics were 27%, 39%, and 63% for **1**–**3**, respectively. From the DSC measurements, hybrid **1** showed the melting transition of the PCL block at 53.3 °C, and the PS glass transition at 88.9 °C (Fig. 2). But, the PEO melting transition was not shown, which suggests that nanoparticles mostly exist in the PEO block. This particle localization in the PEO region might be due to the earlier crystallization of the PCL block. According to several publications, PEO and PCL blocks are well-known to be miscible in the melt [24]. Thus, in an initial stage, the nanoparticles may exist in the mixed PEO/PCL phase. As the residual solvents are evaporated, however, it is probable that the PCL blocks crystallize first to expel the nanoparticles into the amorphous PEO-rich region. This interpretation seems to be plausible by considering the DSC data of hybrid **2** and **3** with higher f_ws, where no PCL melting transition was observed. It might be because more added particles also disturb the PCL crystallization in the mixed PEO/PCL phase.

SAXS and TEM experiments were performed on the hybrid materials to determine their microstructures. The SAXS pattern of **1** showed three reflections with *q*-spacing ratios of 1:2:3, and from the primary peak, its periodic lamellar thickness was estimated to be 30.5 nm (Fig. 3(a)). More details of this lamellar structure could be investigated using TEM experiments. Consistent with the SAXS results, the TEM image of the unstained microtomed film of **1** exhibited a lamellar pattern consisting of three distinct layers,

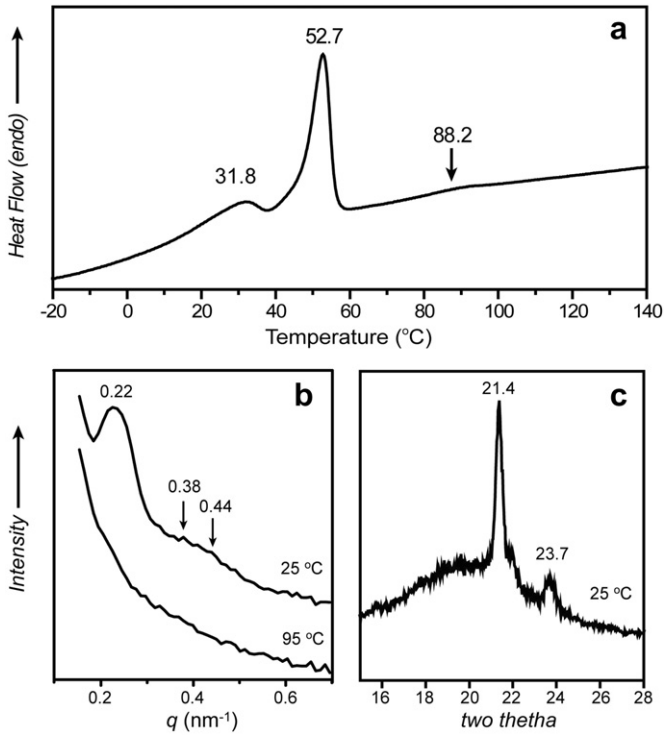

Fig. 1. (a) DSC thermogram (b) SAXS, and (c) WAXS spectra of **PS-*b*-PEO-*b*-PCL**.

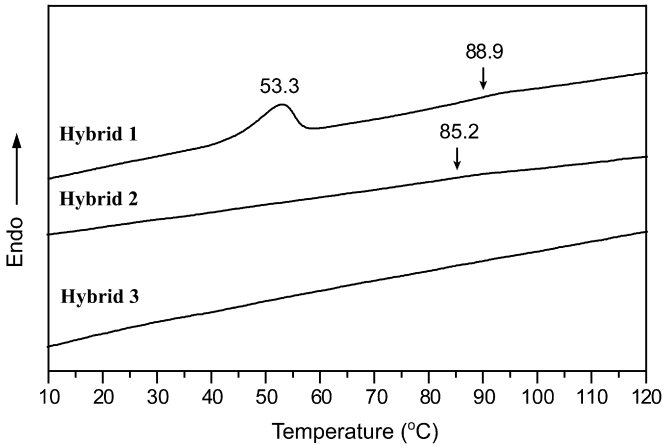

Fig. 2. DSC thermograms of hybrid materials **1**–**3**.

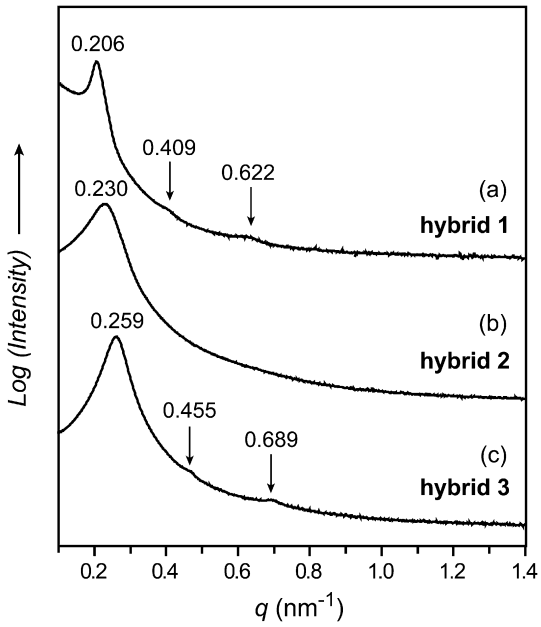

Fig. 3. SAXS spectra of hybrid materials **1**–**3**.

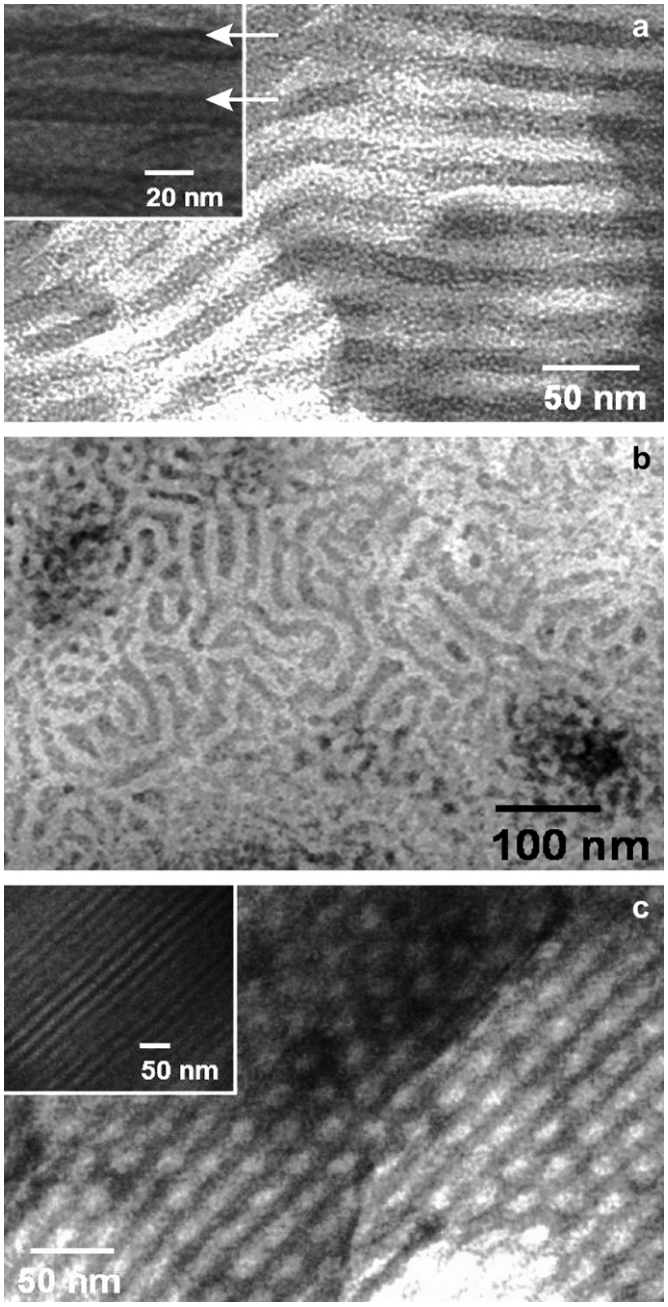

Fig. 4. TEM images of **1**–**3**. (a) Microtomed bulk film of **1**, (b) ultrasonicated bulk sample of **2** in toluene and (c) microtomed bulk film of **3**. In the inset of (a), the darkest regions (See white arrows) are silica layers at the PS/PEO interface.

which correspond to silica (the darkest), PS (the medium dark), and PEO/and PCL (the brightest), respectively (Fig. 4(a)). It is interesting to note that the silica layer is located at the PS/PEO interface. According to the theoretical report about AB block copolymer/particle composites, when the size of loaded nanoparticles is sufficiently smaller than the length of the A polymer block accommodating particles, nanoparticles tend to localize at the AB interface [9,10]. This is because the composite system is dominated by the particle translational entropy. On the other hand, large particles nano-segregate away from the interface; otherwise, a significant loss in the chain conformational entropy happens. From the previous publication, the average diameter of the silica particles used in this study was demonstrated to be less than 5 nm [25]. Consequently, during the formation of the lamellar nanocomposite, small silica particles favor the PS/PEO interface by the dominant particle translational entropy.

In contrast to hybrid **1**, hybrid **2** with $f_w = 0.39$ exhibited no melting transition in its DSC data. This thermal behavior suggests that extra-loaded nanoparticles reside in the mixed PEO and PCL phase, leading to the suppression of PCL crystallization. Therefore, hybrid **2** presumably consists of two different domains, i.e., hydrophobic PS and (PEO + PCL + silica particles). In the SAXS data, hybrid **2** showed only a single reflection, and no higher order reflections were found (Fig. 3(b)). It may indicate that hybrid **2** formed a less regular structure, in comparison to hybrid **1**. So, we examined the TEM images of **2**. The TEM sample was obtained by the dissolution and ultrasonication of the bulk material in toluene. As appears in Fig. 4(b), the TEM image showed a worm-like pattern consisting of regular sized layers. However, a lamellar regularity was frustrated. This TEM data may agree well with the SAXS data. As compared to the lamellar thickness (30.5 nm) of **1**, the primary *d*-spacing (27.3 nm) of hybrid **2** decreased despite the higher loading of nanoparticles. From this, it can be said that the interfacial curvature increased on going from **1** to **2**. In other words, the increased volume by more added nanoparticles expands more horizontally than vertically to the layer plane. One way to explain this might be due to the fact that despite the increased unfavorable interfacial area, the expanded cross-section could alleviate the conformational energy of the long PS coil. So, in order to confirm this argument quantitatively, we analyzed the cross-sectional area of a single PS coil in the layer structure on the basis of the SAXS data and the density of each block. The cross-sectional area could be calculated by dividing the volume (V, the volume including a single triblock copolymer plus silica) by the half of the primary *d*-spacing in the SAXS data. The reason why we used the half value of the primary *d*-spacing is that triblock copolymer-based morphologies are "bilayer" structures. The volume (V, 69.0 nm^3) of hybrid **2** is larger 1.11 times than that (62.1 nm^3) of hybrid **1**, while the cross-sectional area (S) increases by 1.22 times (from 4.1 nm^2 to 5.0 nm^2). Since the lamellar thickness is proportional to V/S, the added nanoparticles dominantly contributed the lateral expansion at the PS/PEO interface. Consequently, it can be said that the

conformation of the PS coil in hybrid **2** becomes less stretched than in hybrid **1**, which would be a driving force for the reduction of the lamellar thickness.

By loading more silica particles, an ordered morphology was revealed in hybrid **3** with f_wv = 0.63. The SAXS data of **3** displayed three reflections which could be indexed as (10), (11) and (21) planes of a 2-dimensional hexagonal columnar structure (Fig. 3(c)). From the primary reflection, the inter-columnar distance (a) was estimated to be 28.0 nm. To corroborate the SAXS result, the thin-sectioned bulk film of **3** was examined via TEM experiments. In Fig. 4(c), the top-view TEM image represents bright, discrete domains surrounded by a dark matrix. The side-view image in the inset is composed of alternating bright cylinders and dark matrix. The inter-columnar distance from the TEM image was measured to be approximately 25–30 nm, which is consistent with the SAXS results. In this columnar morphology, the dark matrix may consist of silica, PEO and PCL, while the bright domains may consist of PS coils. The DSC data in **3**, where the PCL melting transition shown in **1** disappeared, suggests the above-speculation.

As compared to the columnar morphology of the pristine triblock copolymer, the PS location in the columnar structure of hybrid **3** is completely inverted. Consequently, we were able to tune diverse morphologies from the columnar with a PS matrix, lamellar, disordered layer, to columnar with PS cylindrical cores, as a function of the amount of loaded silica nanoparticles.

4. Conclusions

In this study, we synthesized a triblock copolymer, poly(styrene-*b*-ethylene oxide-*b*-caprolactone) copolymer, via sequential anionic and ring-opening polymerizations. The triblock copolymer exhibited an ordered columnar structure with a PS matrix induced by the PCL crystallization. Using the triblock copolymer as a structure-directing agent, three hybrid materials were prepared by a sol-gel process of (3-glycidyloxypropyl) trimethoxy silane and aluminum *sec*-butoxide. As investigated by SAXS and TEM experiments, hybrid **1** with $f_w = 0.27$ exhibited a lamellar morphology. Interestingly, the TEM analysis indicated that silica nanoparticles localized at the PS/PEO interface, which is attributed to the translational entropy effect of the small silica nanoparticles (average diameter < 5 nm). By increasing the loading amount of silica particles, a disordered layer structure was found in hybrid **2** with $f_w = 0.39$. The TEM image of **2** consisted of bright and dark layers with the regular thicknesses. Upon further loading silica particles, hybrid **3** showed a hexagonal columnar morphology where cylindrical PS domains were surrounded by a matrix composed of silica, PEO and PCL.

Acknowledgements

This work was supported by the Core Research Program (2009-0084501) from the National Research Foundation (NRF), a grant from the Fundamental R&D Program for Core Technology of Materials funded by the Ministry of Commerce, Industry and Energy, Republic of Korea, and the Graduate Research Assistantship of Dankook University. We thank the Pohang Accelerator Laboratory (Beamline 10C1), Korea, for use of synchrotron radiation.

References

[1] Soler-Illia GJD, Sanchez C, Lebeau B, Patarin J. Chem Rev 2002;102:4093–138.
[2] Kang C, Kim E, Baek H, Hwang K, Kwak D, Kang Y, et al. J Am Chem Soc 2009;131:7538–9.
[3] Bockstaller MR, Thomas EL. Phys Rev Lett 2004;93:166106.
[4] Lopes WA, Jaeger HM. Nature 2001;414:735–8.
[5] Yeh SW, Wei KH, Sun YS, Jeng US, Liang KS. Macromolecules 2005;38:6559–65.
[6] Kim BJ, Fredrickson GH, Hawker CJ, Kramer EJ. Langmuir 2007;23:7804–9.
[7] Warren SC, Messina LC, Slaughter LS, Kamperman M, Zhou Q, Gruner SM, et al. Science 2008;320:1748–52.
[8] Balazs AC, Emrick T, Russell TP. Science 2006;314:1107–10.
[9] Thompson RB, Ginzburg VV, Matsen MW, Balazs AC. Science 2001;292:2469–72.
[10] Thompson RB, Ginzburg VV, Matsen MW, Balazs AC. Macromolecules 2002;35:1060–71.
[11] Bockstaller MR, Lapentnikov Y, Margel S, Thomas EL. J Am Chem Soc 2003;125:5276–7.
[12] Sohn BH, Choi JM, Yoo S, Yun SH, Zin WC, Jung JC, et al. J Am Chem Soc 2003;125:6368–9.
[13] Bal M, Ursache A, Tuominen M, Goldbach JT, Russell TP. Appl Phys Lett 2002;81:3479–81.
[14] Weng CC, Wei KH. Chem Mater 2003;15:2936–41.
[15] Toombes GES, Mahajan S, Thomas M, Du P, Tate MW, Gruner SM, et al. Chem Mater 2008;20:3278–87.
[16] Toombes GES, Mahajan S, Weyland M, Jain A, Du P, Kamperman M, et al. Macromolecules 2008;41:852–9.
[17] Flouda G, Reiter G, Lambert O, Dumas P. Macromolecules 1998;31:7279–90.
[18] Arnal ML, Balsamo V, López–Carrasquero F, Contreras J, Carrillo M, Schmalz H, et al. Macromolecules 2001;34:7973–82.
[19] Arnal ML, López-Carrasquero F, Laredo E, Müller AJ. Euro Polym J 2004;40:1461–76.
[20] Song J, Cho BK. Polymer (Korea) 2009;33:458–62.
[21] Vangeyte P, Jérôme RJ. Polym Sci Part A Polym Chem 2004;42:1132–42.
[22] He C, Sun J, Ma J, Chen X, Jing X. Biomacromolecules 2006;7:3482–9.
[23] Simon PFW, Ulrich R, Spiess HW, Wiesner U. Chem Mater 2001;13:3464–86.
[24] Castillo RV, Müller AJ. Prog Polym Sci 2009;34:516–60.
[25] Jain A, Wiesner U. Macromolecules 2004;37:5665–70.